LA-UR-01-0175
Approved for public release;
distribution is unlimited.

Title: **A Discrete Multicomponent Fuels Model for GDI Engine Simulations**

Author(s): D.J. Torres, P.J. O'Rourke, A.A. Amsden

Submitted to:

http://lib-www.lanl.gov/la-pubs/00818573.pdf

A Discrete Multicomponent Fuels Model for GDI Engine Simulations

D.J. Torres*, P.J. O'Rourke, A.A. Amsden
Theoretical Division, Los Alamos National Laboratory
Los Alamos, NM 87545 USA

Abstract

We derive equations for multicomponent fuel evaporation, solve the nonlinear equations using Broyden's method, and implement the model into KIVA-3V. A numerical simulation is performed comparing single and multicomponent fuel evaporation.

Introduction

Until recently, most models of fuel sprays and wall films have used a single component fuel [1]. However, flame propagation rate, spray penetration, and fuel chemistry are all functions of fuel composition and vaporization rates [2]. Implementing a multicomponent fuel model would improve the accuracy in predicting these facets of fuel injection and thus overall engine performance.

There exist two different means of modeling multicomponent fuels. In the first, the fuel is modeled as discrete fuel species, the characteristics of which are determined from fuel libraries. In the second model type, the fuel is treated as a continuous species. The fuel composition is described by a probability density function (PDF), and thus fuel properties are deduced from this PDF [2] based on molecular weight, boiling point, or carbon number [3]. While fuels can be composed of hundreds of hydrocarbons, most fuels can be accurately modeled with a few components [4]. For this reason, we have chosen to develop a discrete multicomponent fuel model.

Most discrete fuel studies which assume a finite non-zero mass diffusion rate are performed with binary mixtures, ([5], [6], [7]), and study the effects of Lewis number, Reynolds number, droplet composition, and fuel volatility differences. Zeng and Lee's [8]-[10] discrete model of multicomponent fuel has considered four or more fuel components. They use a transport equation to evolve the difference between surface and average values for temperature as well as species mass fraction. Effective thermal and mass diffusivities are used to account for internal circulation within the droplet. Raoult's law or the Redlich-Kwong equation of state (at high pressures) are used to determine thermodynamical phase equilibrium.

The differences between our model and other discrete models lie in how the Nusselt and Sherwood numbers in both the liquid and gas phases are modeled, the fact that we do not decouple the temperature equations from the species mass fractions equations by neglecting the smaller contributions from the liquid enthalpy diffusion terms and convective term and our use of a temperature dependent pure fuel density. The use of a Broyden iterative scheme allows us to implicitly solve the nonlinear equations that arise when modeling a fuel with many components.

Equations

We begin with the general conservation equations with Fickian diffusion, neglecting external forces, thermal radiation, Soret and Dufour effects, and viscous terms, and derive for a spherically symmetric droplet, a transport equation for the mass of fuel species i,

$$\frac{\dot{M}_i}{4\pi r_s^2} = \rho_{l_s} Y_{g_s,i}(R - v_{l_s})$$

$$+\rho_{g_s} D_{g,i} Sh_{g,i} \left(\frac{Y_{g_\infty,i} - Y_{g_s,i}}{2r_s} \right). \qquad (1)$$

an interface condition for species i,

$$\rho_{l_s}(v_{l_s} - R)(Y_{g_s,i} - Y_{l_s,i})$$

$$+\rho_{l_s} D_{l,i} Sh_{l,i} \left(\frac{Y_{l_s,i} - \bar{Y}_{l,i}}{2r_s} \right)$$

*Corresponding Author

$$-\rho_{g_s} D_{g,i} Sh_{g,i} \left(\frac{Y_{g_\infty,i} - Y_{g_s,i}}{2r_s} \right) = 0, \quad (2)$$

a transport equation for the total internal energy within the droplet,

$$\frac{\dot{\mathcal{I}}_l}{4\pi r_s^2} = \rho_{l_s} I_{l_s} (R - v_{l_s}) - p_l v_{l_s}$$

$$+\lambda_{l_s} Nu_l \left(\frac{T_s - T_d}{2r_s} \right)$$

$$+\rho_{l_s} \sum_i h_{l_s,i} D_{l,i} Sh_{l,i} \left(\frac{Y_{l_s,i} - \bar{Y}_{l,i}}{2r_s} \right), \quad (3)$$

and an interface condition on temperature,

$$\sum_i \dot{M}_i L_{i_s} - 2\pi r_s \left[\lambda_{l_s} Nu_l (T_s - T_d) \right.$$

$$\left. -\lambda_{g_s} Nu_g (T_{g_\infty} - T_s) \right] = 0. \quad (4)$$

One can also show

$$R - v_{l_s} =$$

$$-\frac{\sum_{i_{fuel}} \rho_{g_s} D_{g,i} Sh_{g,i} (Y_{g_s,i} - Y_{g_\infty,i})}{2\rho_{l_s} r_s (1 - Y_{g_s,F})}, \quad (5)$$

by summing (2) over all fuel species, and enforcing,

$$\sum_{i_{fuel}} Y_{l_s,i} = 1, \quad \sum_{i_{fuel}} D_{l,i} \nabla Y_{l_s,i} = 0. \quad (6)$$

In the equations above, $\bar{Y}_{l,i}$ is the mean species mass fraction,

$$\bar{Y}_{l,i} = M_i / M, \quad M = \sum_i M_i, \quad (7)$$

and $Sh_{l,i}$ and $Sh_{g,i}$ are Sherwood numbers within the liquid and gas phase, defined to be,

$$Sh_{l,i} = \frac{\left(\frac{\partial Y_i}{\partial r}\right)_{r_{l_s}}}{\left(\frac{Y_{l_s,i} - \bar{Y}_{l,i}}{2r_s}\right)}, \quad Sh_{g,i} = \frac{\left(\frac{\partial Y_i}{\partial r}\right)_{r_{g_s}}}{\left(\frac{Y_{g_\infty,i} - Y_{g_s,i}}{2r_s}\right)}. \quad (8)$$

Similarly the liquid and gas Nusselt numbers, Nu_l and Nu_g are defined to be

$$Nu_l = \frac{\left(\frac{\partial T}{\partial r}\right)_{r_{l_s}}}{\left(\frac{T_s - T_d}{2r_s}\right)}, \quad Nu_g = \frac{\left(\frac{\partial T}{\partial r}\right)_{r_{g_s}}}{\left(\frac{T_{g_\infty} - T_s}{2r_s}\right)}. \quad (9)$$

In addition, one has the following relations between T_s and I_{l_s} and $\mathcal{I}_l$ and T_d:

$$I_{l_s} = \sum_i Y_{l_s,i} I_{l,i}(T_s), \quad \mathcal{I}_l = \sum_i M_i I_{l,i}(T_d). \quad (10)$$

Here $I_{l,i}$ is the specific internal energy of the pure liquid fuel species i.

One can express $Y_{g_s,i}$ in terms of $Y_{l_s,i}$ using Raoult's law for relatively low pressures. Raoult's law states,

$$p_{g_s,i} = X_{l_s,i} p^o_{vap,i} \ , \quad (11)$$

where $p_{g_s,i}$ is the partial pressure of species i in the gas phase at the droplet surface, and $p^o_{vap,i}$ is the equilibrium vapor pressure for a pure species i. The quantities $X_{l_s,i}$ and $Y_{g_s,i}$ are determined from the relationship between mole and mass fractions.

Using

$$\rho_l = \left(\sum_i \frac{Y_{l,i}}{\rho^o_{l,i}} \right)^{-1} \quad (12)$$

one can derive an equation for the liquid velocity at the droplet surface [8],

$$v_{l_s} = \sum_i \frac{\rho_{l_s} D_{l,i}}{\rho^o_{l,i}} Sh_{l,i} \left(\frac{Y_{l_s,i} - \bar{Y}_{l,i}}{2r_s} \right)$$

$$-\frac{1}{4\pi r_s^2} \frac{dT_d}{dt} \sum_i \frac{M_i}{(\rho^o_{l,i})^2} \frac{d\rho^o_{l,i}}{dT}. \quad (13)$$

We use the following form for the Nusselt number in the gas

$$Nu_g = (2.0 + 0.6 Re_g^{\frac{1}{2}} Pr_g^{\frac{1}{3}}) \frac{\ln(1 + B_d)}{B_d}, \quad (14)$$

where B_d is the fuel Spalding transfer number,

$$B_d = \frac{\sum_{i_{fuel}} Y_{g_s,i} - \sum_{i_{fuel}} Y_{g_\infty,i}}{1 - \sum_{i_{fuel}} Y_{g_s,i}}, \quad (15)$$

Re_g is the Reynolds number and Pr_g is the gas Prandtl number. We also use the following form for the Sherwood number in the gas

$$Sh_{g,i} = (2.0 + 0.6 Re_g^{\frac{1}{2}} Sc_{g,i}^{\frac{1}{3}}) \frac{\ln(1 + B_d)}{B_d}, \quad (16)$$

where $Sc_{g,i}$ is the Schmidt number,

$$Sc_{g,i} = \frac{\mu_{g_\infty}(\hat{T})}{\rho_{g_\infty} D_{g,i}(\hat{T})}. \quad (17)$$

We obtain a transport equation for the actual thermal boundary layer thickness , δ^T by assuming δ^T relaxes to δ^T_{eq} with a relaxation time, τ_{eq}, following Zeng and Lee [10],

$$\frac{d\delta^T}{dt} = \frac{\delta^T_{eq} - \delta^T}{\tau_{eq}}, \quad (18)$$

where

$$\tau_{eq} = \frac{(\delta^T_{eq})^2}{\alpha_l} c_\tau,$$

and c_τ is a constant of $\mathcal{O}(1)$.

We derive a preliminary expression for the equilibrium thermal boundary layer thickness, $\tilde{\delta}^T_{eq}$, of a rapidly vaporizing drop by setting the diffusion wave velocity equal to the surface regression rate

$$\frac{\alpha_l}{\tilde{\delta}^T_{eq}} = c_\delta |R|, \quad (19)$$

where c_δ is a constant of $\mathcal{O}(1)$. In addition, we enforce the restriction $\delta^T_{eq} < \frac{2r_s}{Nu_{lam}}$ on the final equilibrium boundary layer thickness by setting

$$\delta^T_{eq} = \frac{1}{\frac{Nu_{lam}}{2r_s} + \frac{c_\delta |R|}{\alpha_l}}. \quad (20)$$

Once one has solved for the thermal boundary layer thickness, δ^T, the liquid Nusselt number is then set equal to

$$Nu_l = \frac{2r_s}{\delta^T}. \quad (21)$$

We expect that for newly formed droplets from breakup, δ^T should be small, and so we initialize δ^T to be $\delta^T \approx 10^{-5} r_s$.

We derive the liquid Sherwood number by realizing that $Le_l = \frac{\alpha_l}{D_l} = \frac{\delta^T}{\delta^M}$ where δ^M is the concentration boundary layer thickness. Typically $Le_l = \mathcal{O}(10^1 - 10^2)$. Thus δ^M will be smaller than δ^T and there will exist a steep gradient in species mass fraction near the surface of the droplet. Accordingly by (8), we set

$$Sh_{l,i} = Nu_l Le_l. \quad (22)$$

We also typically set $D_{l,i}$ to be equal for all species. Setting the product $Sh_{l,i} D_{l,i}$ to be the same for all species, allows one to enforce both constraints in (6).

To summarize, (1) provides N_s transport equations for the N_s masses M_i, (2) provides N_s equations for the N_s unknown mass fractions, $Y_{l_s,i}$, (3) provides a transport equation for $\mathcal{I}_l$, and (4) provides an equation for T_s. Equation (5) determines the surface regression rate R. One also requires (7), and (10)-(22) which define $\bar{Y}_{l,i}$, I_{l_s}, T_d, $Y_{g_s,i}$, ρ_{l_s}, v_{l_s}, Nu_g, Sh_g, Nu_l, and Sh_l.

Numerical solution

To solve the nonlinear set of equations (1)-(5), we use Broyden's method. Broyden's method is a method akin to the secant method, where an approximate Jacobian matrix (J) or derivative is used to update one's solution [11].

One wishes to find a solution to $\mathbf{F}(\mathbf{x}) = \mathbf{0}$, where $\mathbf{F}$ is a set of nonlinear functions. Given an initial guess $\mathbf{x^o}$, set $A^o = J(\mathbf{x^o}) = \frac{\partial F_i}{\partial x_j}$. Do for k = 0,1, ... :

Solve $A^k \mathbf{s^k} = -\mathbf{F}(\mathbf{x}^k)$ for $\mathbf{s^k}$.

Set $\mathbf{x}^{k+1} = \mathbf{x}^k + \mathbf{s}^k$.

Set $\mathbf{y}^k = \mathbf{F}(\mathbf{x}^{k+1}) - \mathbf{F}(\mathbf{x}^k)$.

Update $A^{k+1} = A^k + \frac{(\mathbf{y}^k - A^k \mathbf{s^k})(\mathbf{s}^k)^T}{(\mathbf{s}^k)^T \mathbf{s}^k}$. The first Jacobian, $J(\mathbf{x^o})$, is not found analytically but approximated with finite differences.

Results

We simulate gasoline with a six component blend (synfuel) composed of 24.5% cyclohexane (b.p. 80^oC), 19.3% iso-octane (b.p. 99^oC), 17.5% toluene (b.p. 110^oC), 17.2% iso-pentane (b.p. 27^oC) , 12.9% ethylbenzene (b.p. 137^oC), and 8.6% n-decane (b.p. 173.4^oC) [4] by implementing these multicomponent spray equations into KIVA-3V. A total of 14.7 milligrams of fuel is injected using 8000 spray parcels for 1.5 milliseconds into an ambient pressure of 1 bar. Mass diffusion coefficients are set to $1 \times 10^{-5} \frac{cm^2}{s}$. The axisymmetric calculation is performed in a 4.8825 cm radial by 7.3 cm vertical domain with 50 radial and 75 vertical computational cells. We compare the time evolution of the total liquid fuel for synfuel with the standard

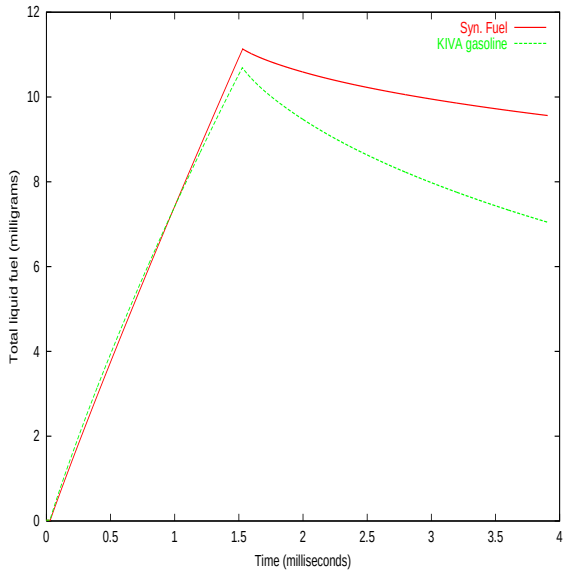

Figure 1: Evolution of total fuel for multi-component fuel blend and standard "KIVA gasoline" at 30^oC

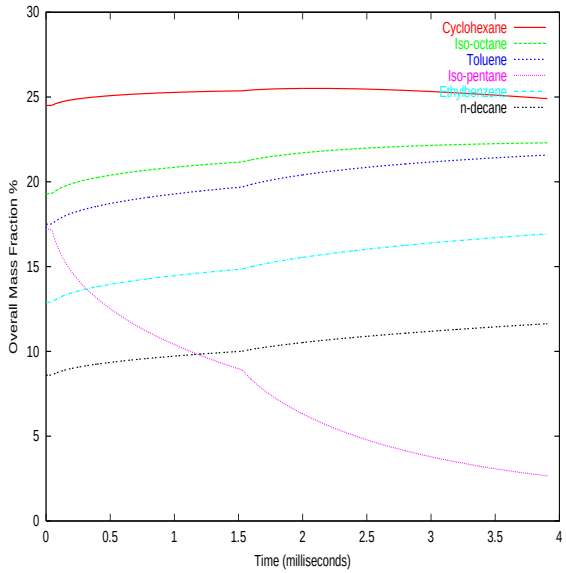

Figure 2: Evolution of species mass fractions for 30^oC injection

"KIVA gasoline" in Fig. 1 for fuel injected at 30^oC. We also display the time evolution of species mass fractions for synfuel for an injection fuel temperature of 30^oC in Fig. 2. We see that synfuel evaporates more slowly than KIVA gasoline in Fig. 1 at least after injection ceases. In Fig. 2, the mass fraction of the most volatile component (iso-pentane) diminishes leaving the less volatile components behind. The mass fraction of cyclohexane (which is the next most volatile component after iso-pentane) initially increases and then decreases gradually during the course of the calculation.

Nomenclature

B_d	Spalding transfer number
D	Mass diffusion coefficient
h	Specific enthalpy
I	Specific internal energy
$\mathcal{I}$	Total internal energy within droplet
L	Latent heat of vaporization
Le	Lewis number
M_i	Mass of species i within droplet
$\dot{M}_i$	$\frac{dM_i}{dt}$
Nu	Nusselt number
N_s	Number of species
p	Pressure
r_s	Droplet radius
R	$\frac{dr_s}{dt}$
Re	Reynolds number
Sc	Schmidt number
Sh	Sherwood number
t	Time
T	Temperature
v	Velocity
v_s	Interfacial velocity
X	Mole fraction
Y	Mass fraction
$\bar{Y}_i$	Mean species mass fraction
ρ	Density
λ	Thermal conductivity
δ^T	Thermal boundary layer thickness
δ^M	Concentration boundary layer thickness
α	Thermal diffusivity
μ	Viscosity

Subscripts

i	Species i
l	Liquid phase
g	Gas phase
l_s	Liquid phase at droplet surface
g_s	Gas phase at droplet surface
∞	Gas phase in droplet cell

References

[1] Amsden, A.A., O'Rourke, P.J., and Butler, T.D., "KIVA-II: A Computer Program for Chemically Reactive Flows with Sprays", Los Alamos National Laboratory Report No. LA-11560-MS UC-96.

[2] Lippert, A.M., Ph.D. Thesis, University of Wisconsin-Madison, 1999.

[3] Tamim, J., and Hallett W.L., *Chemical Engineering Science* 50:2933-2942(1995).

[4] Greenfield, M.L., Lavoie, G.A., Smith, C.S., Curtis, E.W., *SAE 982724.*

[5] Law, C.K., *Prog. Energy Combust. Sci.* 8:171-201 (1982).

[6] Sirignano, W.A., *Fluid Dynamics and Transport of Droplets and Sprays*, Cambridge University Press, 1999, pp 77-92.

[7] Renksizbulut, M., and Bussmann, M., *Int. J. Heat Mass Transfer* 3:2827-2835 (1993).

[8] Zeng, Y., and Lee, C.F., *Journal of Propulsion and Power* 16:964-973(2000).

[9] Zeng, Y., and Lee, C.F., *Internal Combustion Engine Division of ASME 1999 Fall Engine Technology Conference*, Ann Arbor, MI.

[10] Zeng, Y., and Lee, C.F., *SAE 2000-01-0537.*

[11] Dennis, J.E., Schnabel, R.B., *Numerical Methods for Unconstrained Optimization and Nonlinear Equations*, Prentice-Hall, 1983, pp 169-193.